

Chapter 4. Properties of optimized compositional 0.7SrBi₂Ta₂O₉-0.3Bi₃TaTiO₉ solid solution thin films

This chapter includes two sub-chapters. After the optimization process at chapter 4, the properties of the optimized compositional solid solution thin films as a function of their thickness as well as measuring temperature were investigated and discussed. In the section of thickness dependent properties, a possible thin film growth mechanism was discussed. Also, in the section of thermal stability study, the endurance of the solid solution thin films according to the temperature change was studied and compared to other ferroelectric thin films such as Pb(ZrTi)O₃ and SrBi₂Ta₂O₉.

4.1. THICKNESS DEPENDENT PROPERTIES OF 0.7SrBi₂Ta₂O₉-0.3Bi₃TaTiO₉ THIN FILMS

4.1.1 Abstract

The size effect of 0.7SrBi₂Ta₂O₉-0.3Bi₃TaTiO₉ thin films, prepared by metalorganic deposition technique, were studied by determining how the ferroelectric properties vary with film thickness and grain size. It was found that the ferroelectric properties were determined by the grain size, and not by the thickness of the film in our studied thickness range of 80-350 nm. A 80 nm thick film showed good ferroelectric properties similar to the 350 nm thick film. The possible mechanisms for the size effect in 0.7SrBi₂Ta₂O₉-0.3Bi₃TaTiO₉ films are discussed.

4.1.2 Introduction

The size effect of ferroelectric bulk materials have been investigated for several decades.^{1,2} There has been strong interest in the size effects of ferroelectric thin films in recent year, because of their promising nonvolatile memory applications.³⁻⁵ So far, most studies of the size effects in ferroelectric thin films have focused on ABO₃ type materials such as Pb(Zr,Ti)O₃, PbTiO₃, and BaTiO₃. It has been found that the thickness and grain size of the thin film strongly

effect the ferroelectric and optical properties, phase transitions, lattice structure, and stress distribution in ABO_3 type materials.⁶⁻¹⁸ Generally speaking, a reduction in film thickness or grain size leads to a decrease in dielectric constant, remanent polarization, dielectric breakdown field, and the tetragonal distortion c/a , and leads to an increase in loss tangent, coercive field, band gap energy, and diffuseness of the phase transitions.^{7,10}

Several mechanisms for size effects in ferroelectric thin films have been postulated based on the effects of electrodes/film interfacial layers,¹²⁻¹⁴ stresses,¹⁷ defects,¹⁸ and domain structure transitions.¹⁹ The following two models may be the most probable mechanisms for size effects. One is the electrodes/film interfacial layers model.¹²⁻¹⁴ The model assumes that an electrodes/film interfacial layers with low dielectric constant is formed at the interface between the electrode and ferroelectric film by the intrinsic stress during the synthesis process of the film. The low dielectric constant interfacial layers results in a decrease in the effective dielectric constant and remanent polarization, and increase in loss tangent and coercive field of the entire film.¹²⁻¹⁴ The other model is based on the domain structure transition from multidomain predominance to single domain predominance at a critical grain size in the film.¹⁹ The lack of the domain walls and the low domain wall mobility in the single domain predominated film, usually associated with small grains, may induce the size effects.

Recently, layered structure ferroelectric thin films, represented by $SrBi_2Ta_2O_9$, have been intensively studied for their outstanding fatigue free property in nonvolatile memory applications. However, only a little work has been done on the size effects of layered structure ferroelectric thin films.¹³ In this article, $0.7SrBi_2Ta_2O_9-0.3Bi_3TaTiO_9$ film was chosen to study the size effects of the film by determining how ferroelectric properties vary with the film thickness and grain size. Our previous articles²⁰ showed excellent ferroelectric properties for $0.7SrBi_2Ta_2O_9-0.3Bi_3TaTiO_9$ films at a low process temperature of 650 °C, which is about 100 °C lower than usual $SrBi_2Ta_2O_9$ process temperatures.

4.1.3 Experiment

In this study, the $0.7SrBi_2Ta_2O_9-0.3Bi_3TaTiO_9$ thin films were prepared by our modified metalorganic solution deposition (MOD) technique, using an alkoxide-carboxylate precursor solution.²⁰ The films were coated on Pt/Ti/SiO₂/Si substrates by spin coating. Then the films

were kept on a hot plate (at 350 °C) in air for 10 min. The thickness of each coating layer was controlled by adjusting the viscosity of the solution and the spin speed. This step was repeated after each coating to obtain the desired final film thickness of 50, 80, 100, 280, 350 nm. The films were annealed in a tube furnace at temperature of 650 °C for one hour in an oxygen atmosphere to crystallize the films.

The ferroelectric properties were measured by a RT-66 (Radiant Technology Inc.) test system. The dielectric measurements were also conducted by a HP4192A impedance analyzer. Their microstructure was observed by a D3000 atomic force microscope (AFM) (Digital Instrument, Inc), and a Scintag XDS-2000 x-ray diffractometer (XRD) using Cu K_{α} radiation at 40 kV.

4.1.4 Results and Discussion

The films with thickness from 80 to 350 nm showed similar well saturated hysteresis loops, the 50 nm film was electrically shorted. Figure 4-1 shows the hysteresis loop of the film with a thickness of 80 nm. The permanent polarization (P_r) of the 80 nm film has 5 $\mu\text{C}/\text{cm}^2$ and coercive field (E_c) has 63 kV/cm at 2 V and 100 kHz. All the films in the thickness range from 50 to 350 nm showed similar XRD pattern. The XRD pattern indicates that the films were well crystallized. Table 5-1 shows the properties of remanent polarization, coercive field, dielectric constant, and dielectric loss (measured at 100 kHz) as a function of film thickness. The data in Table 4-1 indicates that the electrical properties of the $0.7\text{SrBi}_2\text{Ta}_2\text{O}_9\text{-}0.3\text{Bi}_3\text{TaTiO}_9$ films are independent of film thickness in our studied thickness range. This results are contrary to the reports of piezoelectric (PZT) films, where the electrical properties of PZT films strongly depend on thickness range from 25 to 300 nm.^{6-8, 11, 12}

The films with thickness of 50-350 nm showed similar AFM microstructure. Figure 4-2 shows the AFM microstructure of the 80 nm film. It can be seen in Fig. 4-2 that the film was composed of large stripe shaped grains and small grains. The large stripe shaped grains result in the good ferroelectric properties, and the small grains reduces leakage current to avoid electrical breakdown even in such very thin 80 nm film. A $0.7\text{SrBi}_2\text{Ta}_2\text{O}_9\text{-}0.3\text{Bi}_3\text{TaTiO}_9$ film with a thickness of 350 nm was annealed at 575 °C to obtain grain size of about 50 nm to confirm the

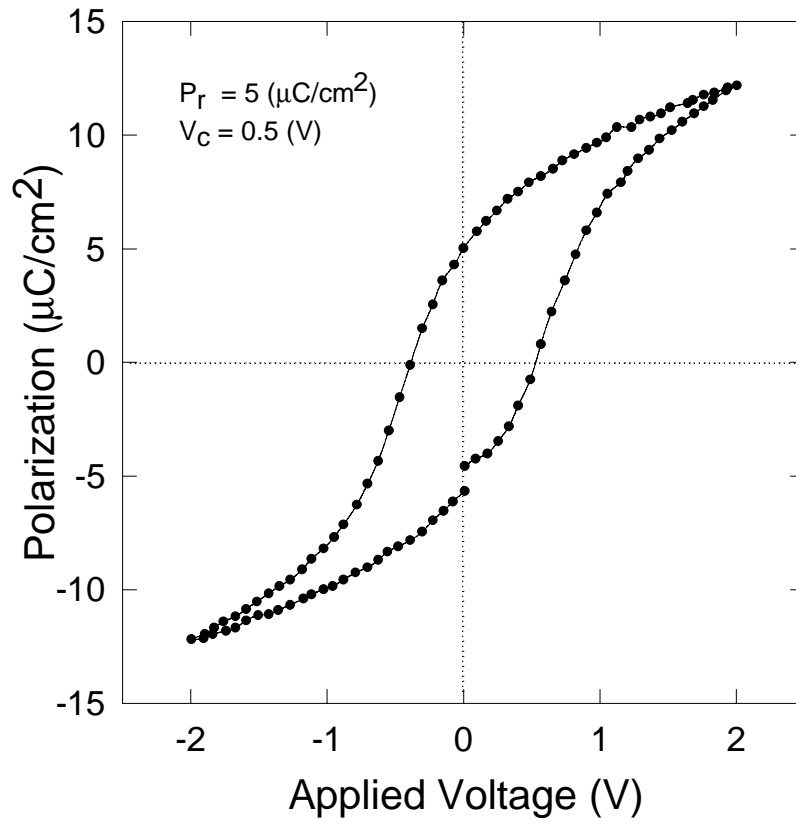
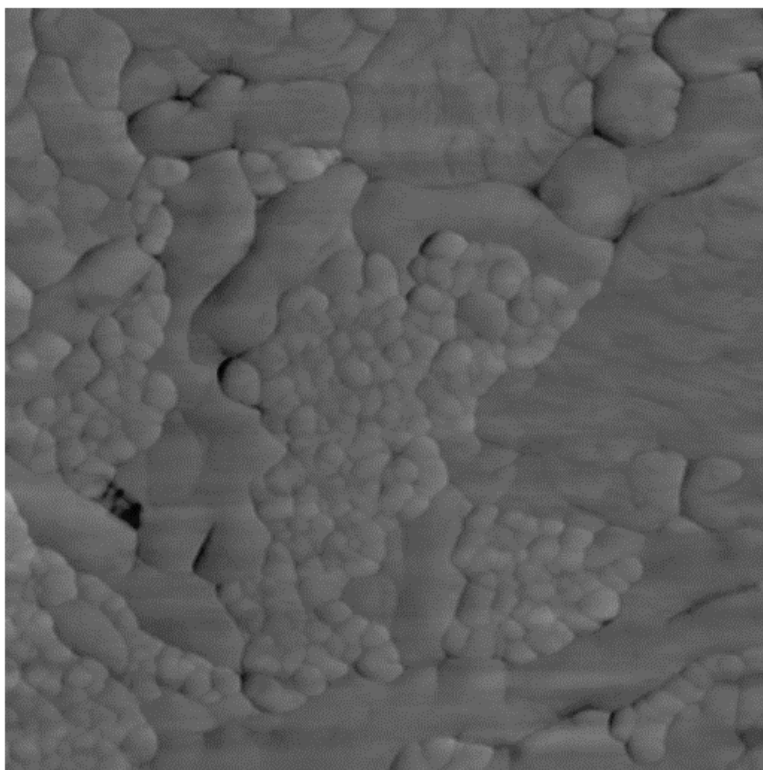


Figure 4-1. Hysteresis loop of $0.7\text{SrBi}_2\text{Ta}_2\text{O}_9\text{-}0.3\text{Bi}_3\text{TaTiO}_9$ film with thickness of 80 nm at 2 V

Table 4-1. Electrical properties of 0.7SrBi₂Ta₂O₉-0.3Bi₃TaTiO₉ thin films with different thickness

Film thickness (nm)	P _r ^a (μC/cm ²)	E _c ^a (kV/cm)	Dielectric constant	Dielectric loss
80	5	63	145	0.022
100	5.6	65	150	0.023
280	5.8	70	152	0.025
350	5.5	71	149	0.024

^a At an applied field of 250 kV/cm



1 μ m x 1 μ m

Figure 4-2. The AFM pictures of $0.7\text{SrBi}_2\text{Ta}_2\text{O}_9\text{-}0.3\text{Bi}_3\text{TaTiO}_9$ film with thickness of 80 nm

role of the grain size in the size effect of the ferroelectric thin films. No ferroelectric properties were obtained in this film. It may be concluded that the grain size rather than the film thickness is the main factor for the size effects in these layered structure $0.7\text{SrBi}_2\text{Ta}_2\text{O}_9\text{-}0.3\text{Bi}_3\text{TaTiO}_9$ films.

As we know, the ferroelectric properties are determined mainly by the ferroelectric domain structure, domain nucleation, and the domain mobility. In transmission electron microscopy (TEM) observation of PbTiO_3 film, Ren *et al.*¹⁹ found that domain structures and domain wall mobility were related to the grain size. The domain structure transition from multidomained predominance to single-domain predominance in PbTiO_3 films occurs when the grain size was below a critical grain size. The single-domain predominated grain is very stable under an external field, so that domain nucleation very difficult. Therefore, no good ferroelectric properties can be obtained in a single-domain predominated film, which usually has small grain. A similar dependence of ferroelectric properties on grain size has been found in $\text{SrBi}_2\text{Ta}_2\text{O}_9$ thin films by M. Nagata and S.B. Desu.²¹ But the difference is that the grain size of $\text{SrBi}_2\text{Ta}_2\text{O}_9$ -based film is mainly determined by process temperature and not by the film thickness. However the grain size of ABO_3 materials is controlled not only by process temperature but also by the film thickness.

Several researchers have reported a linear relationship between the grain size and the film thickness from 25 to 300 nm in ABO_3 type ferroelectric films, such as $\text{Pb}(\text{Zr},\text{Ti})\text{O}_3$ ^{6,8} and PbTiO_3 ¹¹, but this relationship was not observed in layered $\text{SrBi}_2\text{Ta}_2\text{O}_9$ -based thin films. We think that a small tetragonal distortion in ABO_3 type ferroelectric films makes the formation of spherically shaped grains much easier, and causes the grain size to be limited by the film thickness. However, the large difference between interatomic distance of a and c axis in the layered structure thin film causes anisotropic grain growth. Anisotropic grain growth is not limited by the film thickness, and causes the stripe shaped grains (as seen in this article).

4.1.5 Conclusion

A series of $0.7\text{SrBi}_2\text{Ta}_2\text{O}_9\text{-}0.3\text{Bi}_3\text{TaTiO}_9$ thin films with thickness from 50 to 350 nm were fabricated by the MOD method. The size effect of $0.7\text{SrBi}_2\text{Ta}_2\text{O}_9\text{-}0.3\text{Bi}_3\text{TaTiO}_9$ thin films have been studied by comparing ferroelectric properties with film thickness and grain size. It has

been found that the ferroelectric properties were determined by the grain size, and not by the thickness of the film in our studied thickness range of 50-350 nm. In contrast with ABO₃ type materials, the grain size is independent of the film thickness in layered ferroelectric materials. A 80 nm thick 0.7SrBi₂Ta₂O₉-0.3Bi₃TaTiO₉ film showed good ferroelectric properties similar to the 350 nm thick film. We believe that the large difference between the interatomic distance of a and c in the layered ferroelectric materials causes anisotropic grain growth. Anisotropic grain growth results in grain size that is not limited by the film thickness.

4.1.6 References

1. A. Jaccard, W. Kanzig, and M. Peter, *Helv. Phys. Acta* 26, 521 (1953)
2. M. Anliker, H.R. Brugger, and W. Kanzig, *Helv. Phys. Acta* 27, 99 (1954)
3. J.F. Scott and A. Arroyo, *Science* 246, 1400 (1989)
4. M. Sayer and K. Sreenivas, *Science* 247, 1056 (1990)
5. M.H. Francombe and S.V. Krishnaswamy, *J. Vac. Sci. Technol. A* 8, 1382 (1990)
6. S.B. Desu, C.H. Peng, L. Kamnerdiana, and P.J. Schuele, *Mater. Res. Soc. Symp. Proc.* 200, 319 (1990)
7. K.R. Udayakumar, P.J. Schuele, L. Chen, S.B. Krupanidhi, and L.E. Cross, *J. Appl. Phys.* 77, 3981 (1991)
8. M. De Keijser, G.J.M. Dormans, J. Van Veldhover, and De Leeuw, *Appl. Phys. Lett.* 59, 3556 (1991)
9. X.M. Lu, J.S. Zhu, W.Y. Zhang and Y.N. Wang, *Thin Solid Films* 274, 165 (1996)
10. J.S. Zhu, X.M. Lu, W. Jiang, W. Tian, M. Zhu and Y.N. Wang, *J. Appl. Phys.* 81, 1392 (1997)
11. D.M. Tahan, A. Safari and L.C. Klein, *J. Am. Ceram. Soc.* 79, 1594 (1996)
12. Y. Sakashita, H. Segawa, K. Tominaga and M. Okada, *J. Appl. Phys.* 73, 7857 (1993)
13. A. Gilteson, A.M. Lerre, and S.V. Orlov, *Sov. Phys. Solid State* 9, 1121 (1997)
14. P.K. Larsen, G.J.M. Dormans, D.J. Taylor and J. Van Veldhover, *J. Appl. Phys.* 76, 2405 (1994)
15. J.F.M. Cillessen, M.W. Jprins and R.M. Wolf, *J. Appl. Phys.* 81, 2777 (1997)
16. J.W. Jang and S.J. Chung, *J. Appl. Phys.* 81, 6322 (1997)

17. H.D. Chen, K.K. Li, C.J. Gaskey and L.E. Cross, Mater. Res. Soc. Symp. Proc. 433, 325 (1996)
18. S.T. McKinstry, C.A. Randall, J.P. Maria C. Theis, D.G. Schlom, J. Spepard, Jr. and K. Yamakawa, Mater. Res.Soc. Symp. Proc. 433, 363 (1996)
19. S.B. Ren, C.J. Lu, J.S. Liu, H.M. Shen and Y.N. Wang, Phys Rev. B 54, R14 337 (1996); 55, 3485 (1997)
20. X. Zhang, P. Gu and S.B. Desu, Phys. Status Solidi A 160, 35 (1997); S.B. Desu, P.C. Joshi, X. Zhang and S.O. Ryu, Appl. Phys. Lett. 71, 1041 (1997)
21. M. Nagata, D.P. Vijay, X. Zhang and S.B. Desu, Phys. Status Solidi A 157, 75 (1996)
22. S. Hayashi, K. Arita, Y. Shimada, E. Fujii, T.Otsuki and C.A. Paz de Araujo, Ultrathin (,70 nm) Layered perovskite for Megabit-scale FeRAMs in 1.5V Regime, Presented on Nineth International Symposium Integrated Ferroelectrics Santa Fe, New Mexico, USA 2-5 March 1997 (unpublished)

4.2 THERMAL STABILITY OF FERROELECTRIC 0.7SrBi₂Ta₂O₉-0.3Bi₃TaTiO₉ SOLID SOLUTION THIN FILM

4.2.1. Abstract

We have investigated the ferroelectric properties for 0.7SrBi₂Ta₂O₉-0.3Bi₃TaTiO₉ solid solution thin films as a function of temperature. A solid solution of 0.7SrBi₂Ta₂O₉-0.3Bi₃TaTiO₉ thin film was prepared by means of metalorganic deposition method onto platinized silicon. We found that this film shows a stable polarization hysteresis loop at temperatures as high as 200 °C, which is higher than that of Pb(Zr,Ti)O₃ thin film, as well as of SrBi₂Ta₂O₉. The observed remanent polarization ($2P_r$) at 170 °C was 23 $\mu\text{C}/\text{cm}^2$ and showed only a 10 % reduction from its room temperature value. Such thermal stability is believed to be due to lower Schottky barrier height of 0.7SrBi₂Ta₂O₉-0.3Bi₃TaTiO₉ (0.17 eV) as compared to that of Pb(Zr,Ti)O₃ (0.45 eV), assuming that the leakage current of these films are dominated by Schottky emission. A higher Curie temperature of 0.7SrBi₂Ta₂O₉-0.3Bi₃TaTiO₉ (450 °C) than that of SrBi₂Ta₂O₉ (310 °C) may be also responsible for the thermal stability of 0.7SrBi₂Ta₂O₉-0.3Bi₃TaTiO₉.

4.2.2 Introduction

Ferroelectric thin films have been intensively studied over the past few years as candidates for specific microelectronic applications including electrooptic sensors, electromechanical actuators and nonvolatile ferroelectric random access memories (NvFRAMs). Amongst them, Pb(Zr,Ti)O₃ and SrBi₂Ta₂O₉ thin films are the promising NvFRAM materials, for their synthesis and processing techniques as well as electrical characteristics are appreciably established and well understood. Despite their notable ferroelectric properties, the Pb(Zr,Ti)O₃ thin films with conventional Pt electrodes have a serious problem of polarization fatigue and SrBi₂Ta₂O₉ has a demerit of high processing temperature around 750 °C. Desu *et al* have reported that a solid solution of SrBi₂Ta₂O₉, such as (1-x)SrBi₂Ta₂O₉-xBi₃TiNb and (1-x)SrBi₂Ta₂O₉-xBi₃TaTiO₉ showed decent ferroelectric properties at a processing temperature as low as 650 °C¹. In the end, it has been shown that the most suitable ferroelectric properties for the NvFRAM application were obtained at the composition of 0.7SrBi₂Ta₂O₉-0.3Bi₃TaTiO₉.

One of the important properties of NvFRAMs is the stability at high temperatures for the reliable operation of the device as well as for the specific applications which require endurance in the presence of thermal shock. The thermal stability of $\text{Pb}(\text{Zr,Ti})\text{O}_3$ thin film capacitors in 64 kbyte NvFRAMs up to 125 °C was reported by Yoo *et al.*², in that, $\text{Pb}(\text{Zr,Ti})\text{O}_3$ thin films showed pyroelectric effect that may cause the device malfunctioning. Also temperature dependent ferroelectric behavior of $\text{SrBi}_2\text{Ta}_2\text{O}_9$ thin film capacitor was reported by Taylor *et al.*³, where large amount of polarization reduction was observed at temperatures higher than 150 °C. In this chapter, we present the thermal stability of the $0.7\text{SrBi}_2\text{Ta}_2\text{O}_9\text{-}0.3\text{Bi}_3\text{TaTiO}_9$ thin film capacitor, as compared to that of $\text{SrBi}_2\text{Ta}_2\text{O}_9$, as well as of $\text{Pb}(\text{Zr,Ti})\text{O}_3$.

4.2.3 Experimental Procedure

$\text{Pb}(\text{Zr,Ti})\text{O}_3$ thin films with the composition of $\text{Pb}_{1.1}(\text{Zr}_{0.53}\text{Ti}_{0.47})\text{O}_3$ were prepared by the conventional sol-gel method⁴ and the modified metalorganic synthesis method was adopted for the preparation of $\text{SrBi}_2\text{Ta}_2\text{O}_9$ ⁵ and $0.7\text{SrBi}_2\text{Ta}_2\text{O}_9\text{-}0.3\text{Bi}_3\text{TaTiO}_9$ ¹ thin films. To obtain proper ferroelectric properties, 5% of excess bismuth was added to the stoichiometric $\text{SrBi}_2\text{Ta}_2\text{O}_9$ composition. The resultant thickness of the films was determined by means of spectroscopic ellipsometry. The measured $\text{Pb}(\text{Zr,Ti})\text{O}_3$ layer was approximately 230 nm, and 290 nm for the $\text{SrBi}_2\text{Ta}_2\text{O}_9$ and $0.7\text{SrBi}_2\text{Ta}_2\text{O}_9\text{-}0.3\text{Bi}_3\text{TaTiO}_9$ thin films. $\text{Pb}_{1.1}(\text{Zr}_{0.53}\text{Ti}_{0.47})\text{O}_3$ films were annealed at 600 °C for one hour and an annealing temperature of 750 °C was used for $\text{SrBi}_2\text{Ta}_2\text{O}_9$ and $0.7\text{SrBi}_2\text{Ta}_2\text{O}_9\text{-}0.3\text{Bi}_3\text{TaTiO}_9$. The Pt top electrodes of 140 nm in thickness and $3.5 \times 10^{-4} \text{ cm}^2$ in area were sputter-deposited using a shadow mask for all the films, and the films were annealed at 600 °C for 5 min prior to the electrical measurements. The ferroelectric properties were measured by using a RT66A standard ferroelectric tester (Radiant Technologies). Dielectric constant and loss factor were measured by using a LF impedance analyzer (HP 4192A) at 100 kHz at the oscillating level of 10 mV. The measurement of leakage current-voltage (I-V) characteristics was carried out by using a electrometer/source (Keithley 617). The bias voltage, starting from 7 volt, was applied to the grounded bottom electrode with step mode of both delay time and interval time of 60 s and step voltage of -0.2 volt, which could measure only non-switching polarization current excluding any additional poling process in the leakage current measurement. Details of this methods will be described elsewhere⁶.

4.2.4 Results and Discussion

The temperature dependence of the P-E hysteresis behavior was performed using a 3 inch diameter thermal chuck inside a shielding box to preserve constant temperature. A 20 min delay time was applied prior to the each electrical measurement to stabilize the temperature. Figure 4-3 (a)-(c) shows typical temperature dependent P-E hysteresis loops for $0.7\text{SrBi}_2\text{Ta}_2\text{O}_9-0.3\text{Bi}_3\text{TaTiO}_9$, $\text{SrBi}_2\text{Ta}_2\text{O}_9$, and $\text{Pb}_{1.1}(\text{Zr}_{0.53}\text{Ti}_{0.47})\text{O}_3$ thin film capacitors, respectively. As seen in Fig. 4-3 (a), thermal P-E hysteresis behavior of $0.7\text{SrBi}_2\text{Ta}_2\text{O}_9-0.3\text{Bi}_3\text{TaTiO}_9$ is more stable than that of the others. There was no observable decrease of remanent polarization at 170 °C. In the case of $\text{SrBi}_2\text{Ta}_2\text{O}_9$, as shown in Fig. 4-3 (b), remanent polarization at the temperature of 170 °C almost vanishes. On the other hand, the $\text{Pb}_{1.1}(\text{Zr}_{0.53}\text{Ti}_{0.47})\text{O}_3$ thin film showed quite different thermal behavior of the P-E loop different from that of bismuth layered structure materials, as shown in Fig. 4-3 (c). The P-E loops of $\text{Pb}_{1.1}(\text{Zr}_{0.53}\text{Ti}_{0.47})\text{O}_3$ at temperatures of 140 °C showed distorted loop, which is caused by leakage current through the $\text{Pb}_{1.1}(\text{Zr}_{0.53}\text{Ti}_{0.47})\text{O}_3$ body at 140 °C. However, like in the case of $0.7\text{SrBi}_2\text{Ta}_2\text{O}_9-0.3\text{Bi}_3\text{TaTiO}_9$, there was no great change in remanent polarization compared to the value obtained at room temperature.

Figure 4-4 shows that the temperature dependence of the remanent polarization and coercive field of $0.7\text{SrBi}_2\text{Ta}_2\text{O}_9-0.3\text{Bi}_3\text{TaTiO}_9$ and $\text{SrBi}_2\text{Ta}_2\text{O}_9$ capacitors. As shown in Fig 5-4 (a), reduction rate of $2Pr$ value in $0.7\text{SrBi}_2\text{Ta}_2\text{O}_9-0.3\text{Bi}_3\text{TaTiO}_9$ thin film was slower than the one in $\text{SrBi}_2\text{Ta}_2\text{O}_9$. Since those two materials have different Curie temperatures (T_c) it was expected that the polarization loss of $0.7\text{SrBi}_2\text{Ta}_2\text{O}_9-0.3\text{Bi}_3\text{TaTiO}_9$, of which has a phase transition temperature is near 450 °C⁷, is smaller than that of $\text{SrBi}_2\text{Ta}_2\text{O}_9$ when measured at the same temperatures. However, the rate of polarization loss in $\text{SrBi}_2\text{Ta}_2\text{O}_9$ is quite fast in the temperature range which is still lower than its Curie temperature. As pointed out in the case of PbTiO_3 ⁸, the phase transition temperature of the $\text{SrBi}_2\text{Ta}_2\text{O}_9$ thin film may be somewhat altered due to the different thermal expansion coefficient of the platinum substrate and the $\text{SrBi}_2\text{Ta}_2\text{O}_9$ thin film which can cause stress effects on the Curie temperature. In addition, compositional and structural disorder may cause a diffuse phase transition, which was often observed in a ferroelectric relaxor⁹. In fact, the temperature dependent dielectric constant change of the $\text{SrBi}_2\text{Ta}_2\text{O}_9$ thin film reported by Taylor *et al* showed quite a rapid increase of the dielectric constant even at near 100 °C. Since 5% of excess bismuth was used to the stoichiometric $\text{SrBi}_2\text{Ta}_2\text{O}_9$ in this study the

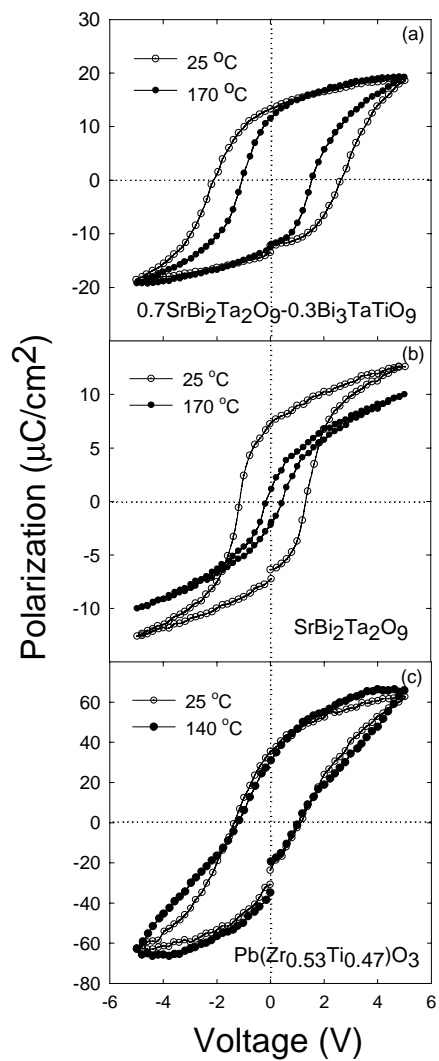


Figure 4-3. Hysteresis loops of (a) $0.7\text{SrBi}_2\text{Ta}_2\text{O}_9-0.3\text{Bi}_3\text{TaTiO}_9$, (b) $\text{SrBi}_2\text{Ta}_2\text{O}_9$ thin films measured at 25 $^\circ\text{C}$ and 170 $^\circ\text{C}$, respectively and (c) $\text{Pb}_{1.1}(\text{Zr}_{0.53}\text{Ti}_{0.47})\text{O}_3$ thin film measured at 25 $^\circ\text{C}$ and 140 $^\circ\text{C}$

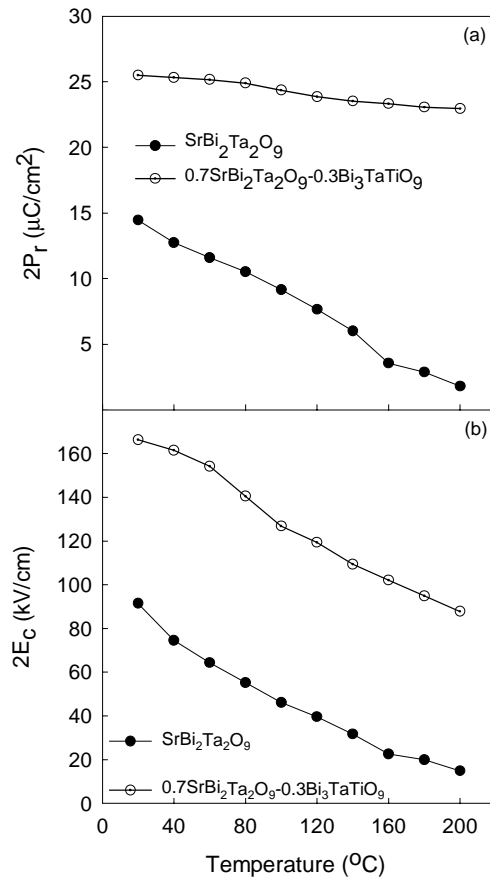


Figure 4-4. Temperature dependent (a) $2P_r$ and (b) $2E_c$ of $0.7\text{SrBi}_2\text{Ta}_2\text{O}_9-0.3\text{Bi}_3\text{TaTiO}_9$ and $\text{SrBi}_2\text{Ta}_2\text{O}_9$ thin films at 5 V

chance of structural disorder in the system is believed to be higher than the stoichiometric $0.7\text{SrBi}_2\text{Ta}_2\text{O}_9\text{-}0.3\text{Bi}_3\text{TaTiO}_9$ thin film. The $2E_c$ values at various temperatures are shown in Fig 4-4 (b). The coercive field ($2E_c$) of the $\text{SrBi}_2\text{Ta}_2\text{O}_9$ thin film almost disappeared at $200\text{ }^\circ\text{C}$, which indicates the film is close to a linear dielectric material due to a phase transition. Although the $0.7\text{SrBi}_2\text{Ta}_2\text{O}_9\text{-}0.3\text{Bi}_3\text{TaTiO}_9$ has a higher Curie temperature, the reduction rate of the coercive field was not much different from $\text{SrBi}_2\text{Ta}_2\text{O}_9$. The temperature dependent coercive field change is considered to be not only a function of Curie temperature but also that of the activation energy of domain wall movement¹⁰. The domains are usually more mobile at a higher temperature, therefore, the coercive field may decrease more rapidly than the change of polarization under a similar temperature range.

The dielectric constant and dissipation factor of the $0.7\text{SrBi}_2\text{Ta}_2\text{O}_9\text{-}0.3\text{Bi}_3\text{TaTiO}_9$ thin film was measured in the temperature range of $25\text{ }^\circ\text{C} - 300\text{ }^\circ\text{C}$. The increase in dielectric constant, as shown in Fig 4-5, was observed but not as rapid as the one of $\text{SrBi}_2\text{Ta}_2\text{O}_9$ thin film². The dielectric constant at $300\text{ }^\circ\text{C}$ was about 350. The $0.7\text{SrBi}_2\text{Ta}_2\text{O}_9\text{-}0.3\text{Bi}_3\text{TaTiO}_9$ thin film also showed a dielectric loss as small as 0.024 at $300\text{ }^\circ\text{C}$. The small dielectric loss at the elevated temperature may attributed to thermally stable ferroelectric properties of $0.7\text{SrBi}_2\text{Ta}_2\text{O}_9\text{-}0.3\text{Bi}_3\text{TaTiO}_9$ thin film.

Figure 4-6(a) shows the leakage current-voltage (J-V) characteristics of the $0.7\text{SrBi}_2\text{Ta}_2\text{O}_9\text{-}0.3\text{Bi}_3\text{TaTiO}_9$ capacitor in the temperature range of $20\text{-}175\text{ }^\circ\text{C}$ by applying DC step voltage from 7V to 0.2V. The space charge effect in J-V curves, as reported by K. Watanabe *et al.*¹¹, was not observed in this study. The reverse step bias method was applied to eliminate the partial switching polarization current in the course of leakage current measurement of the $0.7\text{SrBi}_2\text{Ta}_2\text{O}_9\text{-}0.3\text{Bi}_3\text{TaTiO}_9$ capacitor as well as that of $\text{Pb}(\text{Zr},\text{Ti})\text{O}_3$ and $\text{SrBi}_2\text{Ta}_2\text{O}_9$.⁶ In order to compare the temperature dependent J-V characteristics of $0.7\text{SrBi}_2\text{Ta}_2\text{O}_9\text{-}0.3\text{Bi}_3\text{TaTiO}_9$ to that of $\text{Pb}_{1.1}(\text{Zr}_{0.53}\text{Ti}_{0.47})\text{O}_3$ and $\text{SrBi}_2\text{Ta}_2\text{O}_9$, we chose the leakage current density at 200 kV/cm in the temperature range of $20\text{-}175\text{ }^\circ\text{C}$. Assuming the leakage current density (J) at 200 kV/cm (~ 5 volts) for all test capacitors is dominated by Schottky emission¹², a J/T^2 vs $1/T$ was plotted as shown in Fig. 5-6(b). Each plot in Fig. 4-6(b) shows a straight line with a slope which is related to the Schottky barrier height. The slopes were 0.17 eV, 0.15 eV and 0.45 eV for $0.7\text{SrBi}_2\text{Ta}_2\text{O}_9\text{-}0.3\text{Bi}_3\text{TaTiO}_9$, $\text{SrBi}_2\text{Ta}_2\text{O}_9$ and $\text{Pb}_{1.1}(\text{Zr}_{0.53}\text{Ti}_{0.47})\text{O}_3$, respectively. These values are lower as much as 0.1-0.5 eV than those reported by other groups.^{12, 13, 14} Such a difference may

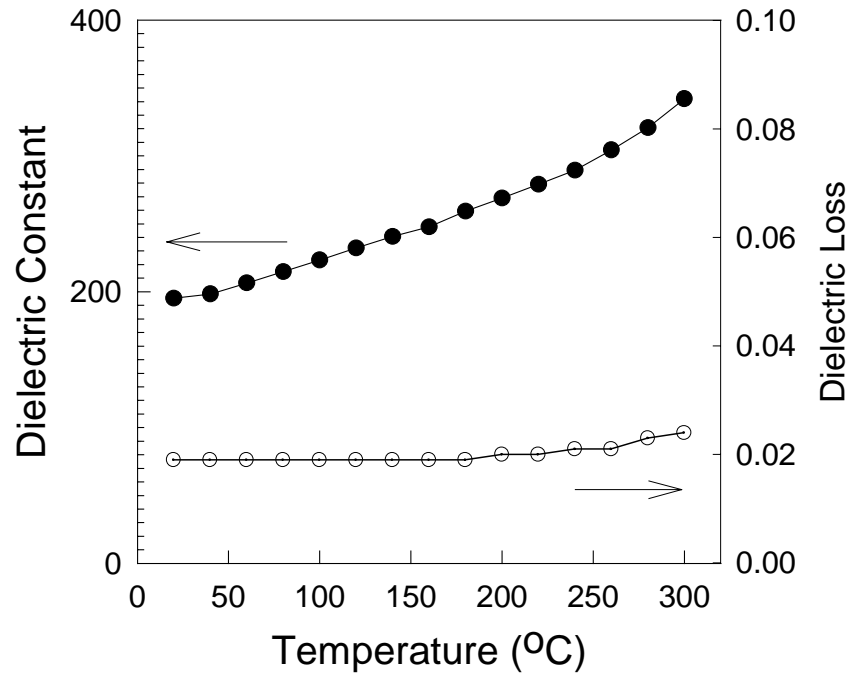


Figure 4-5. Temperature dependence of dielectric constant and loss factor of a $0.7\text{SrBi}_2\text{Ta}_2\text{O}_9$ - $0.3\text{Bi}_3\text{TaTiO}_9$ thin film at the frequency of 100 kHz with 10 mV

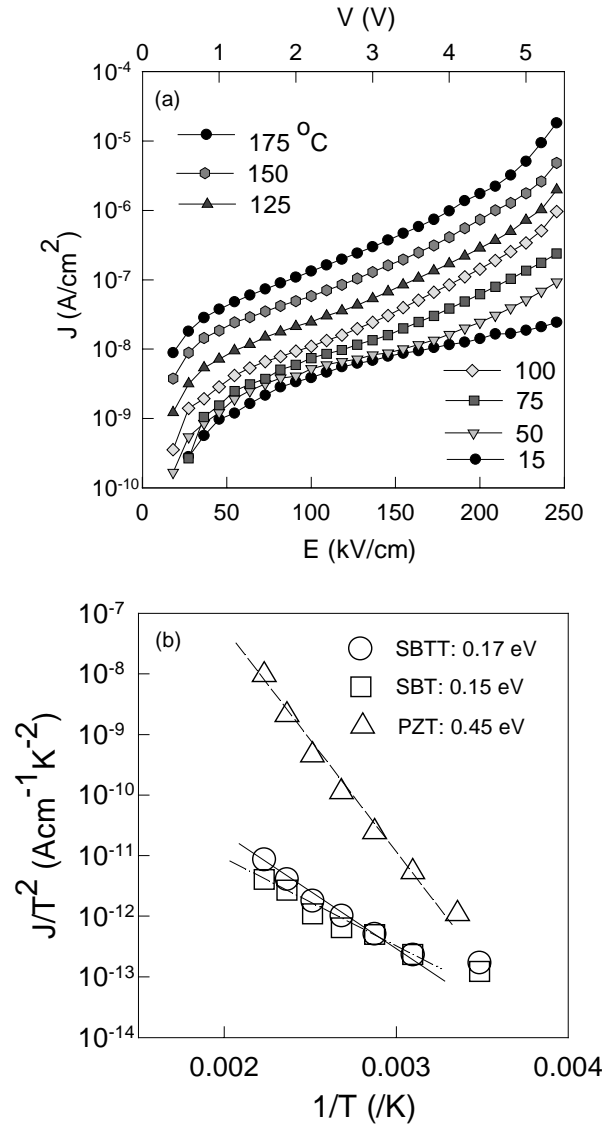


Figure 4-6. A plot of (a) leakage current density (J) vs electric field (kV/cm) for a $0.7\text{SrBi}_2\text{Ta}_2\text{O}_9\text{-}0.3\text{Bi}_3\text{TaTiO}_9$ thin film with temperature range 15 – 175 °C and (b) J/T^2 vs $1/T$ at the electric field of 200 kV/cm for $0.7\text{SrBi}_2\text{Ta}_2\text{O}_9\text{-}0.3\text{Bi}_3\text{TaTiO}_9$, $\text{SrBi}_2\text{Ta}_2\text{O}_9$ and $\text{Pb}_{1.1}(\text{Zr}_{0.53}\text{Ti}_{0.47})\text{O}_3$ thin films

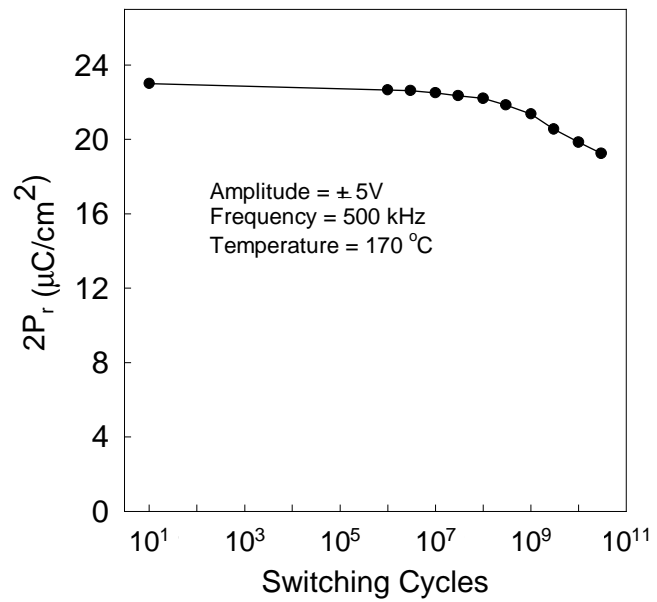


Figure 4-7. Decay in $2P_r$ as a function of number of bipolar switching cycles at the temperature of $170\text{ }^\circ\text{C}$

stems from the different method and the analysis of J-V measurement, which will be discussed in next chapter. From the result of Fig. 4(b), it was observed that the slopes for the $0.7\text{SrBi}_2\text{Ta}_2\text{O}_9-0.3\text{Bi}_3\text{TaTiO}_9$ and $\text{SrBi}_2\text{Ta}_2\text{O}_9$ are less steep than $\text{Pb}_{1.1}(\text{Zr}_{0.53}\text{Ti}_{0.47})\text{O}_3$, indicating the leakage currents of $0.7\text{SrBi}_2\text{Ta}_2\text{O}_9-0.3\text{Bi}_3\text{TaTiO}_9$ and $\text{SrBi}_2\text{Ta}_2\text{O}_9$ are thermally insensitive when compared to that of $\text{Pb}_{1.1}(\text{Zr}_{0.53}\text{Ti}_{0.47})\text{O}_3$. Hence, as it was seen in Fig. 1(c), the leakage current is a dominant phenomenon which governs the thermal stability of $\text{Pb}_{1.1}(\text{Zr}_{0.53}\text{Ti}_{0.47})\text{O}_3$ over the phase transition temperature at 140 °C or above.

The endurance of the $0.7\text{SrBi}_2\text{Ta}_2\text{O}_9-0.3\text{Bi}_3\text{TaTiO}_9$ capacitor at 170 °C was measured by applying 5 V at 500 kHz. As shown in Fig. 4-7, for the switching cycles of up to 10^8 there was no significant fall off in $2P_r$. The onset of fatigue is about 1×10^9 cycles and the $2P_r$ after 10^{10} switching cycles is shown to be a 15 % drop from its initial value.

4.2.5 Conclusion

In conclusion, the thermal behavior of ferroelectric $0.7\text{SrBi}_2\text{Ta}_2\text{O}_9-0.3\text{Bi}_3\text{TaTiO}_9$ solid solution thin films was investigated and compared to other ferroelectric thin film materials such as $\text{Pb}_{1.1}(\text{Zr}_{0.53}\text{Ti}_{0.47})\text{O}_3$ and $\text{SrBi}_2\text{Ta}_2\text{O}_9$. We found that the $0.7\text{SrBi}_2\text{Ta}_2\text{O}_9-0.3\text{Bi}_3\text{TaTiO}_9$ film showed thermal stability in the polarization hysteresis loop at temperatures up to 200 °C, which is better than that of the $\text{Pb}(\text{Zr,Ti})\text{O}_3$ thin film as well as of $\text{SrBi}_2\text{Ta}_2\text{O}_9$. The $2P_r$ and $2E_c$ of the film at 170 °C were $24 \mu\text{C}/\text{cm}^2$ and 83 kV/cm, respectively, with good saturation characteristics. It is seen that both $\text{SrBi}_2\text{Ta}_2\text{O}_9$ and $0.7\text{SrBi}_2\text{Ta}_2\text{O}_9-0.3\text{Bi}_3\text{TaTiO}_9$ have lower leakage current than that of $\text{Pb}_{1.1}(\text{Zr}_{0.53}\text{Ti}_{0.47})\text{O}_3$. The higher Curie temperature (450 °C) of $0.7\text{SrBi}_2\text{Ta}_2\text{O}_9-0.3\text{Bi}_3\text{TaTiO}_9$ may be also responsible for the better thermal stability of the film as compared to $\text{SrBi}_2\text{Ta}_2\text{O}_9$. $0.7\text{SrBi}_2\text{Ta}_2\text{O}_9-0.3\text{Bi}_3\text{TaTiO}_9$ thin film has also shown stable polarization up to 10^9 switching cycles at 170 °C.

4.2.6 References

1. S.B. Desu, P.C. Joshi, X. Zhang, and S.O. Ryu, Appl. Phys. Lett. 71, 1041 (1997)
2. In Kyeong Yoo, I.S. Chung, C.J. Kim, J.K. Lee, B.K. Jeon, and S.B. Desu, MRS Fall meeting Boston (1998)

3. D.J. Taylor, R.E. Jones, P. Zurcher, P. Chu, Y.T. Lii, B. Jiang, and S.J. Gillespie, *Appl. Phys. Lett.* **68**, 2300 (1996)
4. Y. Song, Y. Zhu, and S.B. Desu, *Appl. Phys. Lett.* **72**, 2686 (1998)
5. P.C. Joshi, S.O. Ryu, X. Zhang, and S.B. Desu, *Appl. Phys. Lett.* **70**, 1080 (1997)
6. K.B. Lee, In Kyeong Yoo, S.O. Ryu and S.B. Desu, to be submitted to *Appl. Phys. Lett.*
7. Xubai Zhang, Peizhi Gu, and S.B. Desu, *Phys. Stat. Sol. (a)* **160**, 35 (1997)
8. R.S. Batzer, Bi Ming Yen, Donhang Liu, and Haydn Chen, *J. Appl. Phys.* **80**, 6235 (1996)
9. N. Setter and L.E. Cross, *J. Appl. Phys.* **51**, 4356 (1980)
10. L.I. Dontsova, E.S. Popov, A.V. Shil'nikov, L.G. Bulatova, N.A. Tikhomirova, and L.A. Shuvalov, *Sov. Phys. Crystallogr.* **26**, 430 (1981)
11. K. Watanabe, A.J. Hartmann, R.N. Lamb and J.F. Scott, *J. Appl. Phys.* **84**, 2170 (1998)
12. I. Stolichnov and A. Tangansev, *J. Appl. Phys.* **84**, 3216 (1998)
13. T. Mihara and H. Watanabe, *Jpn. J. Appl. Phys.* **34**, 5564 (1995)
14. C. Sudhama, A.C. Campbell, P.D. Maniar, R.E. Jones, R. Moazzami, C.J. Mogab and J.C. Lee, *J. Appl. Phys.* **75**, 1014 (1994)